DOI:
10.1016/j.jaci.2019.11.030

Document Version
Peer reviewed version

T-cell phenotyping uncovers systemic features of atopic dermatitis and psoriasis.

Consol Farrera, PhD [1,2], Rossella Melchiotti, PhD [2], Nedyalko Petrov, PhD [2], Karen Wei Weng Teng, BSc[3], Michael Thomas Wong, PhD [3], Chiew Yee Loh BSc[3], Federica Villanova PhD [1,2], Isabella Tosi MSc[1,2], Jinmiao Chen, PhD[3], Katarzyna Grys, MSc[1,2], Hemawtee Sreeneebus RGN, MSc[1,2], Anna Chapman MD[4], Gayathri K. Perera PhD, MD[5], Susanne Heck PhD[2], Filipe Gracio PhD[2], Emanuele de Rinaldis PhD [2,+], Jonathan N Barker MD [1], Catherine H. Smith MD [1], Frank O. Nestle MD[1,+], Evan W. Newell PhD [3,*,@,#] and Paola Di Meglio, PhD [1,*,#]

[1]St John's Institute of Dermatology, King's College London, SE1 9RT London, UK. [2]National Institute of Health Research Biomedical Research Centre at Guy's and St Thomas' Hospital and King's College London, London SE1 9RT, UK. [3]Agency for Science Technology and Research (A*STAR), Singapore Immunology Network (SIgN), Singapore 138648, Singapore. [4]Dermatology Department, Queen Elizabeth Hospital, SE18 4QH London. [5]West Middlesex University Hospital, Chelsea and Westminster NHS Foundation Trust, SW10 9NH London. [*]These authors contributed equally to this work.

Present address: + Sanofi, 640 Memorial Drive, Cambridge, MA 02139, USA; @Vaccine and Infectious Disease Division, Fred Hutchinson Cancer Research Center, Seattle, WA, USA.

#Corresponding authors: Paola Di Meglio,
St John's Institute of Dermatology
9th Floor Tower Wing. Guy's Hospital
London SE1 9RT|UK
T:+44-207-188-9068
F:+44-207-188-8050
E: paola.dimeglio@kcl.ac.uk

Evan W Newell
Fred Hutchinson Cancer Research Center
1100 Fairview Ave. N., Mail Stop E5-110
Seattle, WA 98109
T: +1- 206-667-2807
F: +1-206 667-7767
E: enewell@fredhutch.org

Funding Declaration: This research was funded by the National Institute for Health Research (NIHR) Biomedical Research Centre based at Guy's and St Thomas' NHS Foundation Trust and King's College London and/or the NIHR Clinical Research Facility. The views expressed are those of the author(s) and not necessarily those of the NHS, the NIHR or the Department of Health. The authors also acknowledge core funding support (to E.N.) from the Singapore Immunology Network and the Singapore Immunology Network Immune Profiling Platform. E.N. is currently supported by a New Development grant from the Fred Hutchinson Cancer Research Center.

Disclosure of potential conflict of interest: F.O.N and E.d.R. are presently employers of Sanofi. E.N. is a co-founder, share-holder and on the board of directors of Immunoscape Ptd. Ltd. The other authors do not have any relevant competing interest.

Capsule summary:

Deep-immunophenotyping of the circulatory T cell compartment using mass cytometry and unsupervised clustering analysis, identifies phenotypic and functional differences in patients with atopic dermatitis (AD) and psoriasis, highlighting the stronger systemic component associated with AD.

Key Words: mass cytometry, atopic dermatitis, psoriasis, unsupervised analysis, skin inflammation.

Abbreviations:

ANOVA: Analysis of variance

AD: Atopic dermatitis

HD: Healthy donors

F: Functional

P: Phenotypic

DMSO: dimethyl sulfoxide

FOXP3: forkhead box P3

CCR: C C chemokine receptor

TNF: tumor necrosis factor

IFN: interferon

GM-CSF: granulocyte-macrophage colony-stimulating factor

MIP: macrophage inflammatory protein

MR-1: MHC-related protein 1

Th: T helper

CYTOF: Cytometry by time of flight

MAIT: mucosal-associated invariant T

tSNE: t-Distributed Stochastic Neighbor Embedding

PSO: psoriasis

RA: rheumatoid arthritis

T_{RM}: Tissue resident memory T

$T_{CM:}$ central memory T

$T_{EM:}$ effector memory T

$T_{RcM:}$ recirculating memory T

$T_{Reg:}$ Regulatory T

92 **To the Editor**

93

94 Atopic dermatitis (AD) and psoriasis are T cell-mediated, chronic inflammatory skin conditions,
95 which are increasingly recognized as systemic rather than localized cutaneous diseases (1, 2).
96 Hence, a deeper understanding of the phenotypic and functional features of the circulatory T-cell
97 compartment may offer novel insights into their pathogenesis, generate opportunities for novel
98 targeted therapies, as well as, aid in the identification of potential biomarkers. We and others have
99 previously performed fluorescence-based immunophenotyping of circulatory T cells in psoriasis
100 and AD (1), and an earlier comparative study highlighted distinctive features of systemic activation
101 in T cells of AD patients (3). Here, we exploit the increased dimensionality of mass cytometry
102 (cytometry by time of flight, CyTOF), which is able to detect over 50 different heavy metal
103 isotopes simultaneously, and the power of unsupervised analytical methods, to profile and compare
104 phenotypic and functional features of circulating CD4+ and CD8+ T cells of AD (n=15), psoriasis
105 (n=19), and healthy donors (HD, n=9).
106 PBMCs were obtained from a total of 43 age-matched subjects (**Fig. E1A**), recruited into an
107 observational clinical study approved by the London Bridge Research Ethics committee.
108 Demographics and clinical characteristics of the subjects are shown in **Table E1**. A description of
109 the methods is provided in the Methods section in this article's Online Repository at
110 www.jacionline.org.
111 We ran a Phenotypic (P) panel, including 42 lineage, differentiation, activation, trafficking and
112 homing markers, and a Functional (F) panel, including 27 phenotypic surface markers and 15
113 intracellular functional markers (e.g. cytokines, chemokines) (**Table E2**). Frequency of manually
114 gated CD4+ and CD8+ T cells, as well as other major cell populations (**Fig. E1B**), did not
115 significantly differ among AD, psoriasis and HD (**Fig. E1C**). Appling unsupervised clustering
116 analysis to gated CD4+ and CD8+, we identified 144 cell clusters: 34 cell clusters in the CD4+ P

and 31 in the CD8+ P dataset, as well as 51 in the CD4+ F and 29 in the CD8+ F dataset (**Fig. E1A, Fig. E2A**). Each dataset was visualized by applying a dimensionality reduction method, i.e. t-Distributed Stochastic Neighbor Embedding (tSNE) and coloring the cells according to the clusters they were assigned to. Clusters were curated and assigned to standard immune subsets, based on the mean expression of subset-defining markers, such as CD161 and Vα7.2 for mucosal-associated invariant T (MAIT) cells and CD103 for Recirculating memory T cells (T_{RcM}) (**Fig. E2A, Fig. E3-6**).

We compared the average clusters' frequency within each of the four datasets and the means for each cytokine/chemokine in two-way comparisons applying False Discovery Rate (FDR) correction for multiple testing. Overall, we detected statistically significant differences (p-adj < 0.05) in 68 two-way comparisons **(Table E3).** Three cell populations were of particular interest: MAIT cells, T_{RcM} CD8+ T cells, and CD49+ CD4+ Regulatory T (T_{Reg}) cells.

Clusters CD8+P13 and CD8+ F14 displayed the hallmark features of MAIT cells, with high levels of Vα7.2 and CD161 (**Fig. 1A**). Frequencies of MAITs were significantly reduced in psoriasis patients *versus* HD and AD (**Fig. 1B**). This is in keeping with the reported reduction in circulating MAITs in immune-mediated and autoimmune diseases such as RA, where they are correspondingly enriched in the synovial fluid, possibly contributing to disease pathogenesis either directly, or through recruitment of other cells (4). Thus, MAIT cells might preferentially migrate from blood into the inflamed skin, and they have been indeed identified in lesional psoriatic skin (5), although it is not known whether they are increased in inflamed *versus* healthy skin.

The vast majority of MAIT cells produced MIP1-β and TNF (**Fig. 1C, E7A**), with AD producing significantly more than psoriasis (**Fig. 1D, E7B**), suggesting that they are more activated in allergic disease. As MAIT cells respond to MR-1-restricted vitamin B2 derivatives, and *Staphylococcus aureus* is equipped with the specific biosynthetic pathway for their production, their increased activation in AD might be linked to *S. aureus* infection.

Three CD8+ cell clusters identified in both Phenotypic and Functional dataset, i.e. *i*) CD8+ P24/CD8+ F28, *ii*) CD8+ P15/CD8+ F18, and *iii*) CD8+ P27/CD8+ F29, were characterized by the simultaneous expression of low levels of CCR7, and either skin-(CLA+, CCR4+, CCR10+) or gut- (Intb7, CD49d as well as CCR9) homing markers (**Fig. 1E**). Features of these clusters broadly map to effector memory T cells; both skin and gut-homing clusters expressed CD103, suggesting that they previously resided in the tissue, as recently reported for CD4+ CD103+ cells by *Klicznik et al* (6). They may be en-route back from their target organ where they had acquired CD103 expression through exposure to TGF-β of epithelial origin (6). Hence, we tentatively named them T_{RcM}. T_{RcM} were functionally characterized by widespread production of TNF and sizable expression of IL-2, GM-CSF and IL-22 **(Fig. 1F** and **E7C**). Frequencies of all T_{RcM} clusters were significantly increased in AD as compared to HD and psoriasis (**Fig. 1G and E7D**), confirming and expanding recent studies showing increased recirculation, frequency and activation of skin-homing T cells in AD (7). This is in keeping with the sequelae of non-cutaneous atopic manifestations known as atopic march. Of particular interest is the increase in gut-homing T_{RcM}, as AD often precedes the development of food allergy.

Skin- homing T_{RcM} (F28) were the major IL-22 producer within CD8+T cells (**Fig. 1H**), with AD patients producing significantly more IL-22 than HD (**Fig. 1I**). Interestingly, IL22 production in Skin- homing T_{RcM}, correlated with AD severity **(Fig. 1J)**, highlighting the importance of IL-22 in the pathophysiology of AD, and in line with the beneficial effect of IL-22 blockade in AD clinical trials (8).

Lastly, three clusters within the CD4+ Phenotypic dataset displayed hallmarks of T_{Reg} cells: CD45RA+CD45RO- FOXP3+ CD25+ CD127- naïve T_{Reg} (P10), CD45RA-, CD45RO+, CD95+, FOXP3+ CD25+ CD127- CLA+ skin-homing memory T_{Regs} (P14), and CD45RA-, CD45RO+, CD95+, FOXP3+ CD25+ CD127- CD49d+ memory T_{Reg} (P22) (**Fig. 2A**).

Frequencies of P22 memory T_{Reg} were significantly reduced in AD *versus* psoriasis, with a downward trend versus HD (**Fig. 2B**). Earlier studies have reported increased frequency of T_{Reg} in the blood of AD patients (9), although less phenotypic markers have been used, raising the question of whether they were *bona fide* T_{Regs} or a mixed population comprising activated-effector T cells and $T_{Reg.}$ Discrepancies among studies could also be explained by their dynamic fluctuation between the blood and skin compartment potentially driving disease relapses and remissions. This notion is supported by a previous report of Treg frequecny correlating with disease severity (3) although we did not find this relationship in our data (data not shown). To validate our findings, we combined clusters P10, P14 and P22 and performed a zoomed-in tSNE analysis (**Fig. E7E**). While CD45RA, CCR4 and CLA clearly separated T_{Regs} into three clusters (**Fig. E7E**), the presence of additional cell subsets within cluster P14 was also evident, with dichotomous expression of CLA and CD49d in P22 and P14(**Fig. E7F**). Thus, we applied manual gating to further phenotype memory T_{Reg} based on their expression of CLA, CD49d and CCR6. (**Fig. 2C**). AD patients displayed an overall reduced frequency of non-skin homing CD49d+ T_{Reg}, irrespective of CCR6 expression, as compared to psoriasis, and with a downward trend *versus* HD, mirroring the observed decrease in cluster P22. Moreover, CCR6+T_{Reg} within skin-homing CLA+ cells were also significantly reduced in AD *versus* HD, while CCR6-T_{Reg} within skin-homing CLA+ cells were significantly increased in psoriasis *versus* AD and HD (**Fig. 2C**). In contrast, non-T_{Reg} memory CLA+CCR6+ cells were significantly increased in AD as compared to HD and psoriasis.

Here, we have provided an exhaustive description of the circulatory T cell compartment, highlighting phenotypic and functional differences in patients with AD and psoriasis. Unsupervised analysis has overcome the bias of subjective gating by increasing resolution and capturing unexpected combinations of markers, e.g. identifying cell types that escape standard classification strategies, e.g. T_{RcM} expressing CD103.

Our data highlight the stronger systemic component associated with AD, as compared to psoriasis, and provide a resource to further investigate the phenotypic and functional features of the two major inflammatory skin diseases. Future studies are needed to delineate the relationship of the specific cell populations in blood and skin, explore their pathogenic potential, and ultimately assess the utility of these findings for the identification of prognostic and/or predictive biomarkers, as well as potential novel therapeutic targets. Our study proposes MAIT cells as of potential pathogenic relevance for skin inflammation and calls for further studies aimed at assessing their functional capacity in blood and skin of patients with inflammatory skin diseases. IL-22-producing skin-homing T_{RcM} may be an attractive candidate for future studies to identify biomarkers of response to IL-22 blockade in AD. Finally, this study highlights the utility of blood and the use of profiling T cells by trafficking receptor expression patterns for discovery in the context of tissue-specific immunological diseases.

Consol Farrera, PhD [1,2];
Rossella Melchiotti, PhD [2];
Nedyalko Petrov, PhD [2];
Karen Wei Weng Teng, BSc [3];
Michael Thomas Wong, PhD [3];
Chiew Yee Loh, BSc [3];
Federica Villanova PhD, [1,2];
Isabella Tosi MSc [1,2];
Jinmiao Chen, PhD [3];
Katarzyna Grys, MSc [1,2];
Hemawtee Sreeneebus RGN, MSc [1,2];
Anna Chapman MD Queen Elizabeth Hospital;
Gayathri K. Perera, PhD, MD [5];
Susanne Heck, PhD [2]

Filipe Gracio, PhD [2]

Emanuele de Rinaldis, PhD [2, +]

Jonathan N Barker MD, [1]

Catherine H. Smith MD, [1]

Frank O. Nestle MD, [1, +]

Evan W. Newell, PhD, [3,@, *]

Paola Di Meglio, PhD [1,*]

From: [1]St John's Institute of Dermatology, King's College London, SE1 9RT London, UK. [2]National Institute of Health Research Biomedical Research Centre at Guy's and St Thomas' Hospital and King's College London, London SE1 9RT, UK. [3]Agency for Science Technology and Research (A*STAR), Singapore Immunology Network (SIgN), Singapore 138648, Singapore. [4]Dermatology Department, Queen Elizabeth Hospital, SE18 4QH London. [5]West Middlesex University Hospital, Chelsea and Westminster NHS Foundation Trust, SW10 9NH London. [*]These authors contributed equally to this work.

Present address: [+] Sanofi, 640 Memorial Drive, Cambridge, MA 02139, USA; [@]Vaccine and Infectious Disease Division, Fred Hutchinson Cancer Research Center, Seattle, WA, USA.

Corresponding authors: Paola Di Meglio, paola.dimeglio@kcl.ac.uk

Evan W. Newell, enewell@fredhutch.org

Acknowledgements: We would like to thank Laura Turner for her support, critical to the completion of this study. We also would like to thank all patients and healthy volunteers participating to the BIODIP study and the clinical teams at Guy's and St Thomas', Queen Elizabeth and West Middlesex Hospitals.

References:

1. Di Meglio P, Villanova F, Nestle FO. Psoriasis. Cold Spring Harb Perspect Med. 2014;4(8).
2. Weidinger S, Novak N. Atopic dermatitis. Lancet. 2016;387(10023):1109-22.
3. Czarnowicki T, Malajian D, Shemer A, Fuentes-Duculan J, Gonzalez J, Suarez-Farinas M, et al. Skin-homing and systemic T-cell subsets show higher activation in atopic dermatitis versus psoriasis. J Allergy Clin Immunol. 2015;136(1):208-11.
4. Cho YN, Kee SJ, Kim TJ, Jin HM, Kim MJ, Jung HJ, et al. Mucosal-associated invariant T cell deficiency in systemic lupus erythematosus. J Immunol. 2014;193(8):3891-901.
5. Teunissen MBM, Yeremenko NG, Baeten DLP, Chielie S, Spuls PI, de Rie MA, et al. The IL-17A-producing CD8+ T-cell population in psoriatic lesional skin comprises mucosa-associated invariant T cells and conventional T cells. J Invest Dermatol. 2014;134(12):2898-907.
6. Klicznik MM, Morawski PA, Hollbacher B, Varkhande SR, Motley SJ, Kuri-Cervantes L, et al. Human CD4(+)CD103(+) cutaneous resident memory T cells are found in the circulation of healthy individuals. Sci Immunol. 2019;4(37).
7. Czarnowicki T, Santamaria-Babi LF, Guttman-Yassky E. Circulating CLA(+) T cells in atopic dermatitis and their possible role as peripheral biomarkers. Allergy. 2017;72(3):366-72.
8. Guttman-Yassky E, Brunner PM, Neumann AU, Khattri S, Pavel AB, Malik K, et al. Efficacy and safety of fezakinumab (an IL-22 monoclonal antibody) in adults with moderate-to-severe atopic dermatitis inadequately controlled by conventional treatments: A randomized, double-blind, phase 2a trial. J Am Acad Dermatol. 2018;78(5):872-81 e6.
9. Reefer AJ, Satinover SM, Solga MD, Lannigan JA, Nguyen JT, Wilson BB, et al. Analysis of CD25hiCD4+ "regulatory" T-cell subtypes in atopic dermatitis reveals a novel T(H)2-like population. J Allergy Clin Immunol. 2008;121(2):415-22 e3.

Figure Legends

Figure 1: Mucosal-invariant T-cells (MAIT) and Recirculating memory CD8$^+$ T cells in skin disease

(A) Heatmap of mucosal-invariant T (MAIT) cells, within CD8+ Phenotypic and Functional datasets. **(B)** Frequency of MAIT cells in atopic dermatitis (AD), healthy donor (HD) and psoriasis (PSO). **(C)** MIP-1β, TNF-α, IFN-γ, GM-CSF, IL-2 and IL-17A production in MAIT cells, visualized in tSNE. **(D)** Cytokine production in MAIT cells, in AD, HD and PSO. **(E)** Heatmap of recirculating memory T cells (T_{RcM}), within the CD8+ Phenotypic and Functional datasets. **(F)** TNF-α, GM-CSF, IL-2 and IL-22 production in T_{RcM}, visualized in tSNE. **(G)** Frequency of T_{RcM} in AD, HD and PSO. **(H)** Representative dot plots of AD, HD and PSO depicting expression of IL-22 and GM-CSF in manually gated cells (red) within skin-homing T_{RcM} (bottom) compared to total CD8+ T cells (top). **(I)** IL-22 and GM-CSF production in skin-homing $T_{RcM,}$ in AD, HD and PSO. **(J)** Correlation between IL-22 production in skin =homing T_{RcM} and disease severity in AD . Relative cell frequency (B, G) or cytokine expression (D, I) are shown, with circles representing individual samples, and box and whiskers denoting minimum and maximum values.

**p-adj*<0.05; ***p-adj*<0.01

Figure 2. **Regulatory CD4+ T cells in skin disease.**

(A) Heatmap of Regulatory T cells (T_{Regs}), within the CD4+ Phenotypic dataset. **(B)** Frequency of T_{Regs} in atopic dermatitis (AD), healthy donor (HD) and psoriasis (PSO) samples. Relative cell frequency is shown, with circles representing individual samples, and box and whiskers denoting minimum and maximum values. **(C)** Manual gating strategy to obtain Tregs subsets. Differences in cell frequencies were assessed by one -way ANOVA

followed by Dunn test for multiple correction, ****$p\text{-}adj$<0.0001, ***$p\text{-}adj$<0.001, **$p\text{-}adj$<0.01, *$p\text{-}adj$<0.05.

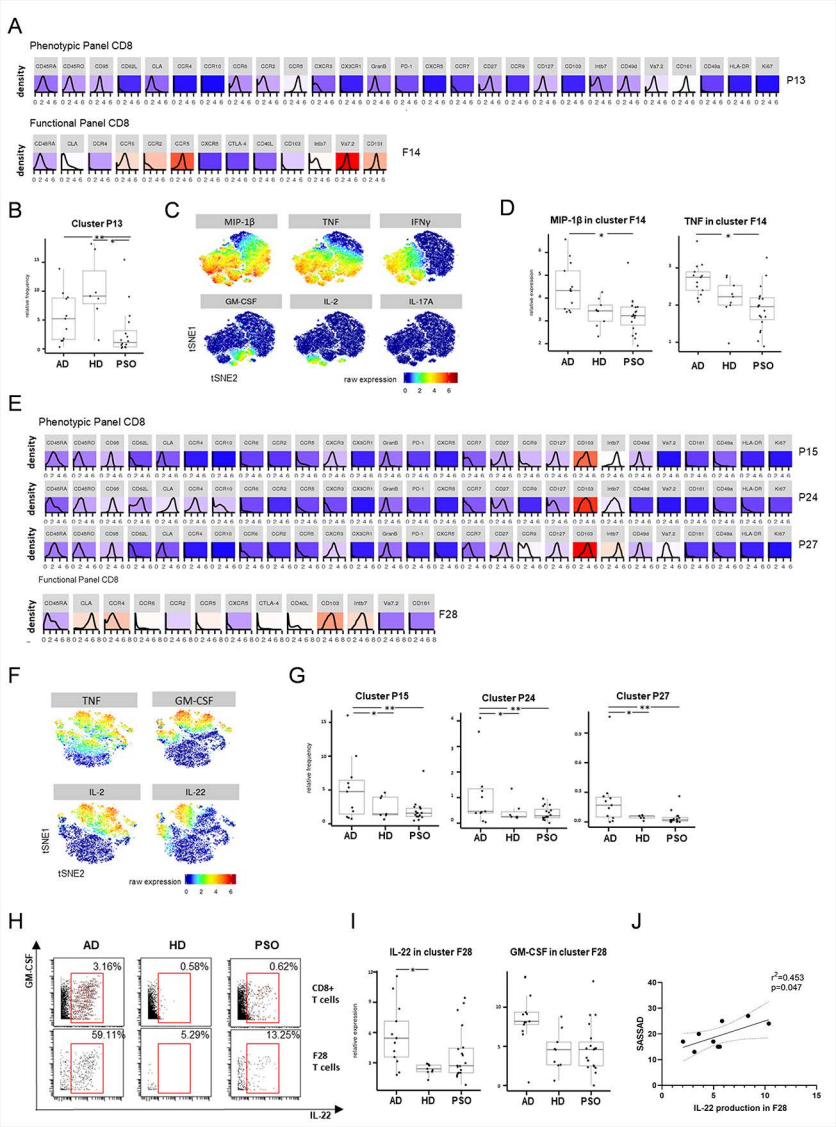
A
Phenotypic Panel CD8
density
CD45RA CD45RO CD95 CD62L CLA CCR4 CCR10 CCR6 CCR2 CCR5 CXCR3 CX3CR1 GranB PD-1 CXCR5 CCR7 CD27 CD9 CD127 CD103 Intb7 CD49d Va7.2 CD161 CD49a HLA-DR Ki67
P13
Functional Panel CD8
CD45RA CLA CCR4 CCR6 CCR2 CCR5 CXCR5 CTLA-4 CD40L CD103 Intb7 Va7.2 CD161
F14
B
Cluster P13
relative frequency
AD HD PSO
C
MIP-1β
TNF
IFNγ
GM-CSF
IL-2
IL-17A
tSNE1
tSNE2
raw expression
D
MIP-1β in cluster F14
TNF in cluster F14
relative expression
AD HD PSO
E
Phenotypic Panel CD8
P15
P24
P27
Functional Panel CD8
F28
F
TNF
GM-CSF
IL-2
IL-22
tSNE1
tSNE2
raw expression
G
Cluster P15
Cluster P24
Cluster P27
relative frequency
AD HD PSO
H
AD HD PSO
GM-CSF
IL-22
3.16%
0.58%
0.62%
59.11%
5.29%
13.25%
CD8+ T cells
F28 T cells
I
IL-22 in cluster F28
GM-CSF in cluster F28
relative expression
AD HD PSO
J
r²=0.453
p=0.047
SASSAD
IL-22 production in F28

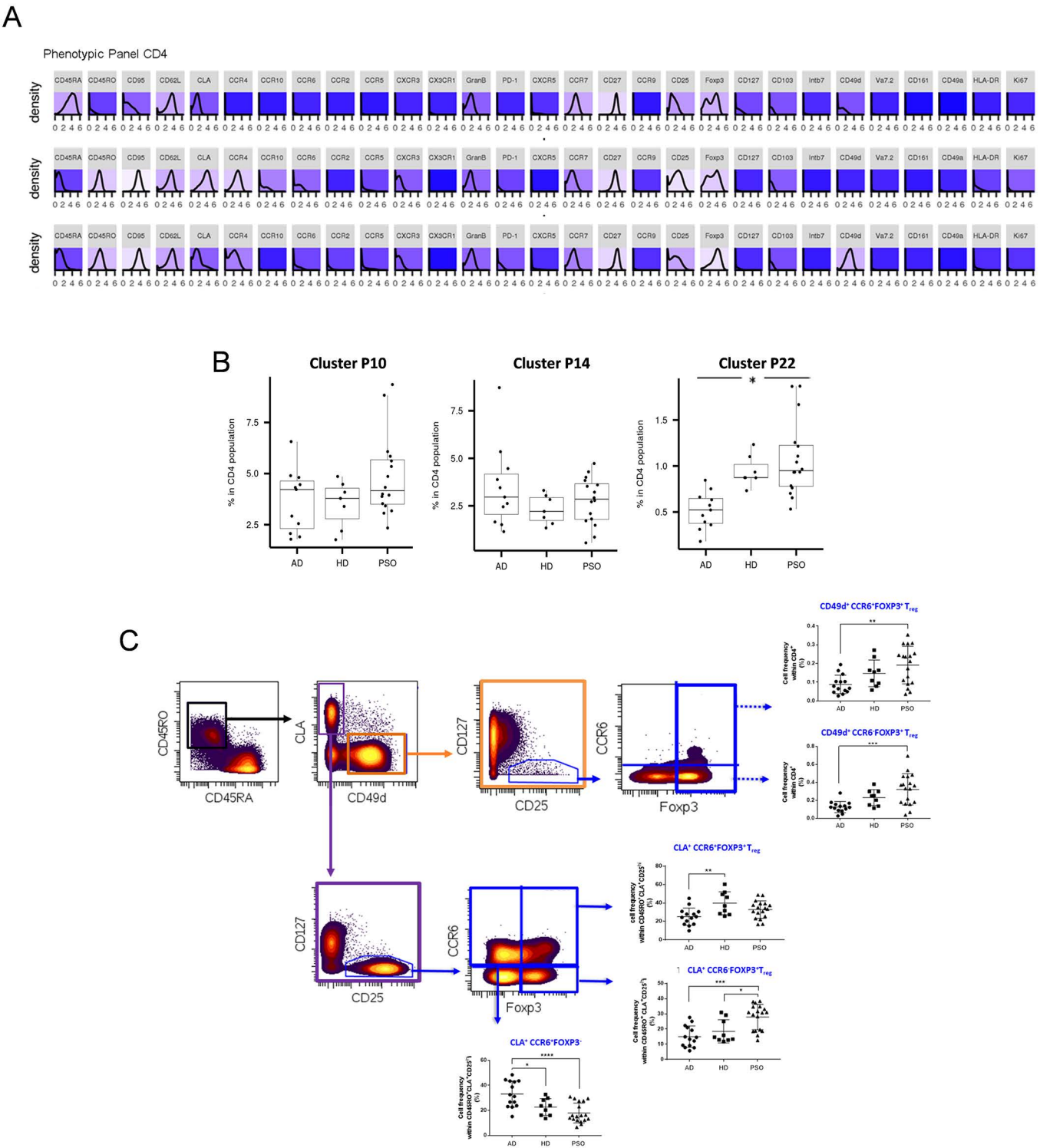
A
Phenotypic Panel CD4
density
CD45RA CD45RO CD95 CD62L CLA CCR4 CCR10 CCR6 CCR2 CCR5 CXCR3 CX3CR1 GranB PD-1 CXCR5 CCR7 CD27 CD9 CD25 Foxp3 CD127 CD103 Intb7 CD49d Va7.2 CD161 CD49a HLA-DR Ki67
P10
P14
P22
B
Cluster P10
Cluster P14
Cluster P22
% in CD4 population
AD HD PSO
C
CD45RO
CD45RA
CLA
CD49d
CD127
CD25
CCR6
Foxp3
CD49d+ CCR6+FOXP3+ Treg
CD49d+ CCR6-FOXP3+ Treg
CLA+ CCR6+FOXP3+ Treg
CLA+ CCR6-FOXP3+ Treg
CLA+ CCR6+FOXP3-
Cell frequency within CD4+ (%)
Cell frequency within CD45RO+CLA+CD25hi (%)

Supplementary Material for Online Repository

T-cell phenotyping uncovers systemic features of atopic dermatitis and psoriasis.

Farrera et al.

Online Methods

Study population

Nine HD, 19 psoriasis and 15 AD patients, recruited at tertiary referral centers at Guy's and St Thomas' Hospital, Queen Elizabeth Hospital and West Middlesex University Hospital, were included in this study. Patients were not receiving any conventional or biological systemic therapy at the time of sampling. Healthy donors were nominally healthy at the time of sample collection and did not report any allergic or auto-immune disease. Full demographics can be found in **Table E1**. The study was conducted in accordance with the Declaration of Helsinki Principles, with written informed consent obtained from each volunteer and approved by the London Bridge Research Ethics committee (Reference 11/LO/1962). One additional healthy donor was recruited at SIgN, A*STAR (IRB number: NUS-IRB-09-256) as internal control to be run with each batch.

PBMCs isolation and cryopreservation

PBMCs were isolated by blood centrifugation on a density gradient (Ficoll-Plaque Plus, VWR). Cells were viably frozen in RPMI 1640 (Life Technologies) supplemented with 11.25% HSA (Gemini Bio-Products)/10% DMSO (Sigma), stored in liquid nitrogen and shipped all together to SIgN A*STAR in a shipper tank filled with liquid nitrogen. PBMCS from one additional healthy donor to be used as internal control (IC) were isolated at the SIgN, A*STAR and cells were

cryopreserved in 90% fetal bovine serum (FBS) (Life Technologies) plus 10% DMSO (MP Biomedicals).

PBMCs stimulation and staining

PBMCS were processed in 7 batches, each including the IC and samples from each BioDiP group (HD, AD and Pso). Cryopreserved cells were thawed, washed with pre-warmed RPMI 1640 supplemented with 1% FBS, 1X Penicillin/Streptomycin/L-glutamine, 1% 1M HEPES and 1X β-mercaptoethanol (all Life Technologies), and rested overnight at 37°C. Next, cells were washed and split into two aliquots of up to 3 x 10^6 cells each for staining with the Phenotypic Panel, including 42 surface and intracellular markers, and the Functional Panel, including 27 phenotypic markers and 14 cytokines (**Table E2**). For both panels, staining of surface markers (Surface I in Table E2) that are weakly expressed or are downregulated during polyclonal stimulation, was carried out in 96-well round bottom plates at 37°C for 30 minutes. Next, cells were either left untreated (Phenotypic Panel) or stimulated with 150 ng/ml phorbol-12-myristate-13-acetate (PMA) and 1 μM ionomycin (Sigma-Aldrich) in the presence of monensin and Brefeldin A (all eBioscience) for four hours for the detection of intracellular cytokines (Functional Panel). After incubation, cells were washed twice in cold PBS, incubated on ice with 100 μM cisplatin (Sigma-Aldrich) for 5 minutes for Live/Dead staining, washed with staining buffer and stained with fluorophore-tagged antibodies for 30 minutes on ice (Surface II, **Table E2**). Next, cells were washed twice in staining buffer and stained with metal isotope-labeled surface antibodies (Surface II, **Table E2**) for 30 minutes on ice.

Cells for the Phenotypic Panel were then washed, fixed in Foxp3 Transcription Factor Fixation/Permeabilization buffer (eBioscience), washed in Permeabilization buffer (Biolegend) and stained with metal isotope-labeled antibodies against intracellular phenotypic markers (Intra

Table E2, Phenotypic Panel), each step carried out on ice for 30 minutes. Next, cells were incubated with metal isotope-conjugated streptavidin for 10 minutes, washed and fixed in 2% paraformaldehyde (PFA; Electron Microscopy Sciences) at 4°C, overnight. Next day, cells were washed twice with 1X perm buffer, once with PBS, and incubated with cellular barcodes for 30 minutes (Surface III, **Table E2**). Next, cells were washed once with 1X perm buffer, incubated in staining buffer for 10 minutes on ice, and DNA was labelled with 250 nm iridium intercalator (Fluidigm Corporation) in PBS-2% PFA at room temperature for 20 minutes. Finally, cells were washed twice with staining buffer, re-suspended in 90% FBS + 10% DMSO in a 96-well round bottom plate and stored immediately at -80°C, prior to CyTOF acquisition.

Following Surface II staining, cells for the Functional Panel were washed twice with staining buffer, once in PBS and fixed in 2% PFA with at 4°C overnight. Next day, cells were washed twice with 1X perm buffer and stained with intracellular antibodies (Intra, **Table E2**, Functional Panel) on ice for 30 minutes. Next, cells were washed, labelled with cellular barcodes and DNA intercalator, cryopreserved and stored until CyTOF acquisition, as described for the Phenotypic Panel.

Cytometry by-time-of-flight (CYTOF)

Prior to CyTOF acquisition, cryopreserved stained cells from each batch were thawed, washed twice and re-suspended in staining buffer. Aliquots of cells from all samples within a batch were pooled and filtered through a 0.35 μm strainer into a 5 ml polystyrene tube. Pooled, filtered cells were washed twice in water before final re-suspension in water at 0.5 x 10^6 cells/ml. EQ Four Element Calibration Beads (Fluidigm Corporation) were added to a concentration of 1% prior to acquisition. Cells acquisition was performed on a CyTOF2 mass cytometer (Fluidigm Corporation).

Data cleaning and manual gating

Raw data were manually cleaned and curated. Patient AD6 was excluded from the overall analysis for low cell viability. Samples run in batch 1 were excluded for unsupervised analysis of the Phenotypic Panel due to suboptimal staining (**Table E1**). Data were normalized with beads and files corresponding to the same batch were concatenated, using the Fluidigm CyTOF software. Obvious dead cells were removed to facilitate debarcoding. Manual debarcoding using Infinicyt software was performed to obtain the individual FCS files for each sample. Manual gating to identify CD4+ and CD8+ T populations for each sample was performed using Cytobank (**Fig. E1B**). From this step onward, each panel (Phenotypic and Functional) and each manually gated T cell compartment (CD4+ T, CD8+ T) was pre-processed, processed for clustering and analyzed independently, resulting in 4 different datasets, Functional CD4, Functional CD8, Phenotypic CD4 and Phenotypic CD8.

T cell datasets pre-processing, QC and clustering

For each dataset, 10,000 CD4+T or CD8+T cells were randomly selected from each sample (or the entire sample was used if it contained less than 10,000 cells) and merged into a single FCS file. Marker expression for all markers except Time and Event length, was asinh-transformed using a cofactor of 5. In order to minimize batch differences, a normalization step was applied to both Panels. For the Functional Panels, CD4+ and CD8+ T-cells were normalized dividing the expression of each marker (except Time, Event length and DNA) by the mean of that marker in the intact live cells from the corresponding batch. In the Phenotypic Panel, CD4 and CD8 T-cells were normalized dividing the expression of each marker by the 99th percentile of that marker in the intact live cells from the corresponding batch. Independent clustering for each of the 4 datasets was performed using the clustering algorithm PhenoGraph in its python implementation (1). The

specific marker combinations, and values of the parameter *k*, the number of nearest neighbor used to build the similarity graph, used for each dataset are listed in **Table E4**.

Quality of normalization and clustering was assessed by visualizing the frequency of each cluster in the IC and 9 HD. Minimal instability was observed among the IC across different batches, while variability among HD was much larger, as expected for true biological variation, which we confirmed by comparing the coefficient of variation of IC and HD ($p<0.001$ for all 4 datasets) (**Fig. E2B** and data not shown).

Dimensionality reduction, visualization and cluster interpretation

Dimensionality-reduction for visualization purposes was performed using the t-Distributed Stochastic Neighbor Embedding algorithm (2) as implemented in the R package *Rtsne*. Representative tSNE plots for each of the 4 datasets were built by randomly selecting 60.000 cells from each dataset. The perplexity parameter was set to 30. The median tSNE1 and tSNE2 coordinates of the cells belonging to each cluster are shown as black dots and labeled by their cluster ID. To enhance visualization, cells were colored according to the clusters they were assigned to. As expected, cells belonging to a specific, colour-coded cluster were found on adjacent coordinates in the tSNE plots (Fig E2A). Additional tSNE plots representative for specific clusters were created by randomly selecting 30.000 cells belonging to those clusters. The perplexity parameter was set to 30 and only cytokines were used to generate the tSNE plots.

Each cluster was manually analyzed and assigned to standard immune subsets, based on the mean expression of subset-defining markers, such as CD161 and Vα7.2 for mucosal-associated invariant T (MAIT) cells and CD103 for Recirculating memory T cells (T_{RcM}) (**Fig. E3A)**. To confirm that the markers used were reliable discriminators for the indicated populations, we combined the profile of selected clusters with the tSNE projection and colour-graded the expression of the most

defining markers for each cell population on the tSNE plot **(Fig E3B)**. As expected, maximal expression of the defining markers co-localized with the tSNE coordinates of the respective cluster shown in **Fig. E2A**. Moreover, visual inspection of density dot plots further confirmed that identified cell cluster were real biological entities, when compared with a negative control population cluster CD8+ F20.

IgE Measurement

IgE were measured in the serum of AD patients using Human IgE Ready-Set-GO from Affymetrix according the manufacturer's instructions.

Statistical Analysis

Frequencies per sample were computed for all clusters in each of the four datasets. Variability within IC and HD was evaluated by calculating coefficient of variation (CV) for each cluster within both groups and performing Mann-Whitney U test comparison for each dataset. Mean normalized expression values for each cytokine per sample in each cluster were also computed for the Functional Panel dataset. Statistical significance for differences in frequencies and mean normalised expression across groups was computed using a linear mixed effects model based on the following formula (in the coding language R):

expression/frequency ~ study_group * visit_number + age + sex + ethnicity + batch +

(1|subject_ID)

That is, where the subject ID represents the random effect variable, and the other variables (including the interaction term between study_group and visit_number) are fixed effects.

Models were fitted using the R package lmer and contrasts of interest were extracted using the function glht from the R package multcomp. This method was chosen to account for the fact that

multiple samples were coming from the same donor and as there were missing samples for some of the time points (where a paired test would have required to drop out many samples). p-values were corrected for the number of clusters (frequency) or cluster-cytokine pairs (mean normalised expression) tested using the Benjamini-Hochberg procedure. For manually gated populations differences were assessed by one-way ANOVA followed by Tukey's test for multiple correction. Correlation between IL-22 production and disease severity in AD patients, measured by SASSAD, was assessed by two-tailed Pearson correlation.Tests with a corrected p-value lower than 0.05 were considered significant

Supplementary References

E1. Levine JH, Simonds EF, Bendall SC, Davis KL, Amir el AD, Tadmor MD, et al. Data-Driven Phenotypic Dissection of AML Reveals Progenitor-like Cells that Correlate with Prognosis. Cell. 2015;162(1):184-97.
E2. van der Maaten L, Hinton G. Visualizing Data using t-SNE. J Mach Learn Res. 2008;9:2579-605.

Supplementary Figure Legends

Figure E1: T cell profiling in inflammatory skin disease

(A) Experimental workflow for the analysis of CD4+ and CD8+ T cells of atopic dermatitis (AD), healthy donor (HD) and psoriasis (PSO) patients by mass-cytometry. PBMCs were stained for phenotypic markers (Phenotypic Panel) or stimulated with PMA/Ionomycin and stained for cytokine production (Functional panel). Four datasets were obtained by pooling manually gated CD4+ or CD8+ cells from each experiment and performing unsupervised clustering analysis. Differential analysis of frequencies and cytokine expression levels was then performed. (B) Gating strategy used to manually identify major cell populations within PBMCs samples. Representative plots shown are from the Phenotypic panel. (C) Pie charts showing mean percentages of main lymphocyte populations within CD45+ cells identified in the Phenotypic panel in AD, HD and PSO.

Figure E2: Evaluation of clusters frequency within healthy donors and internal control

(A) tSNE plots of colour-coded T cell clusters within CD4+ and CD8+ T cells, identified in the Phenotypic and Functional panels. Labelled black dots represent the centroid (based on median) of the corresponding cluster. (B) Evaluation of cluster frequency within healthy donor and Internal control. Bar-plots of relative cluster frequency of 9 healthy donors (HD) and one internal control (IC) run each time, within CD4+ Phenotypic, CD4+ Functional, CD8+ Phenotypic, and CD8+Functional datasets.

Figure E3: Cell clusters identified in the Functional CD8 dataset

(A) Marker analysis and attribution of the 29 clusters identified within the CD4+ Phenotypic dataset to standard cell populations. Normalized expression of all cells assigned to each cluster is represented by colors in the heatmap, and non-normalized raw values are shown as histograms. (B) MAIT and Recirculating Memory T cells identified within the CD8+ Functional dataset are visualized on tSNE plot coloured using normalized values of selected markers (left), and as dot-plots in black (right). Cluster F20, shown in blue, is the negative control.

Figure E4: Cell clusters identified in the CD4+ Functional dataset

Marker analysis and attribution of the 51 clusters identified within the CD4+ Functional dataset to standard cell populations. Normalized expression of all cells assigned to each cluster is represented by colours in the heatmap, and non-normalized raw values are shown as histograms.

Figure E5: Cell clusters identified in the CD4+ Phenotypic dataset

Marker analysis and attribution of the 34 clusters identified within the CD4+ Phenotypic dataset to standard cell populations. Normalized expression of all cells assigned to each cluster is represented by colours in the heatmap, and non-normalized raw values are shown as histograms.

Figure E6: Cell clusters identified in the CD8+ Phenotypic dataset

Marker analysis and attribution of the 31 clusters identified within the CD8+ Phenotypic dataset to standard cell populations. Normalized expression of all cells assigned to each cluster is represented by colours in the heatmap, and non-normalized raw values are shown as histograms.

Figure E7. MAIT, Recirculating memory CD8+ T and T regulatory CD4+ T cells in inflammatory skin disease

A) tSNE visualization of cytokine expression in Functional CD8+ cluster F14 using pooled cells from AD, HD and psoriasis. (B) Cytokine production in cluster F14, in AD, HD and psoriasis. (C) tSNE visualization of cytokine and PD-1 expression in the Functional CD8+ cluster F28 using pooled cells from AD, psoriasis and HD. (D) Box plot showing frequency of TRcM clusters F18, F29 and F29 in the Functional CD8+ dataset. (E) TRegs in clusters P10, P14 and P22 in the CD4+ Phenotypic dataset were merged and coloured by cluster, or according to the raw expression of the indicated markers (F). * $p \leq 0.05$.

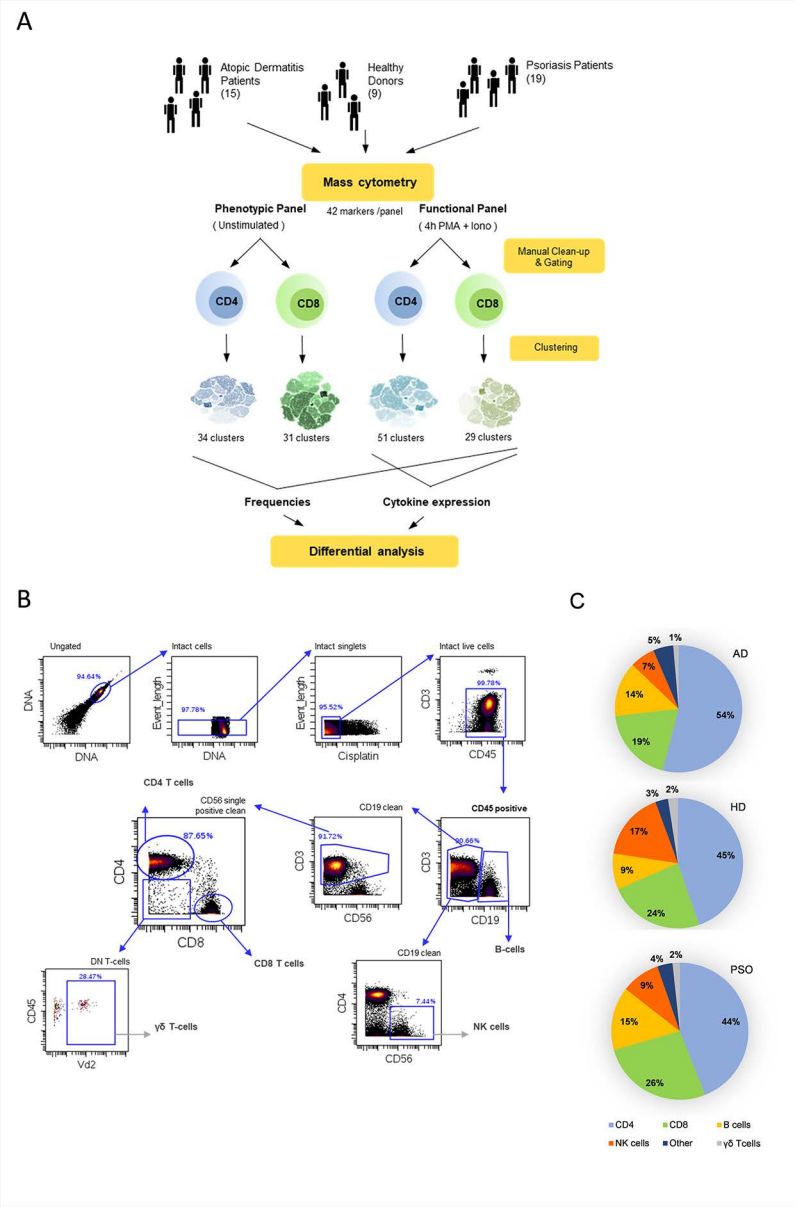
A
Atopic Dermatitis Patients (15)
Healthy Donors (9)
Psoriasis Patients (19)
Mass cytometry
Phenotypic Panel (Unstimulated)
42 markers /panel
Functional Panel (4h PMA + Iono)
Manual Clean-up & Gating
CD4
CD8
CD4
CD8
Clustering
34 clusters
31 clusters
51 clusters
29 clusters
Frequencies
Cytokine expression
Differential analysis
B
Ungated
94.64%
DNA
DNA
Intact cells
97.78%
Event_length
DNA
Intact singlets
95.52%
Event_length
Cisplatin
Intact live cells
99.78%
CD3
CD45
CD4 T cells
CD56 single positive clean
87.65%
CD4
CD8
CD8 T cells
CD19 clean
91.72%
CD3
CD56
CD45 positive
90.66%
CD3
CD19
B-cells
DN T-cells
28.47%
CD45
Vd2
γδ T-cells
CD19 clean
7.44%
CD4
CD56
NK cells
C
AD
5%
1%
7%
14%
54%
19%
HD
3%
2%
17%
45%
9%
24%
PSO
4%
2%
9%
15%
44%
26%
CD4
CD8
B cells
NK cells
Other
γδ Tcells

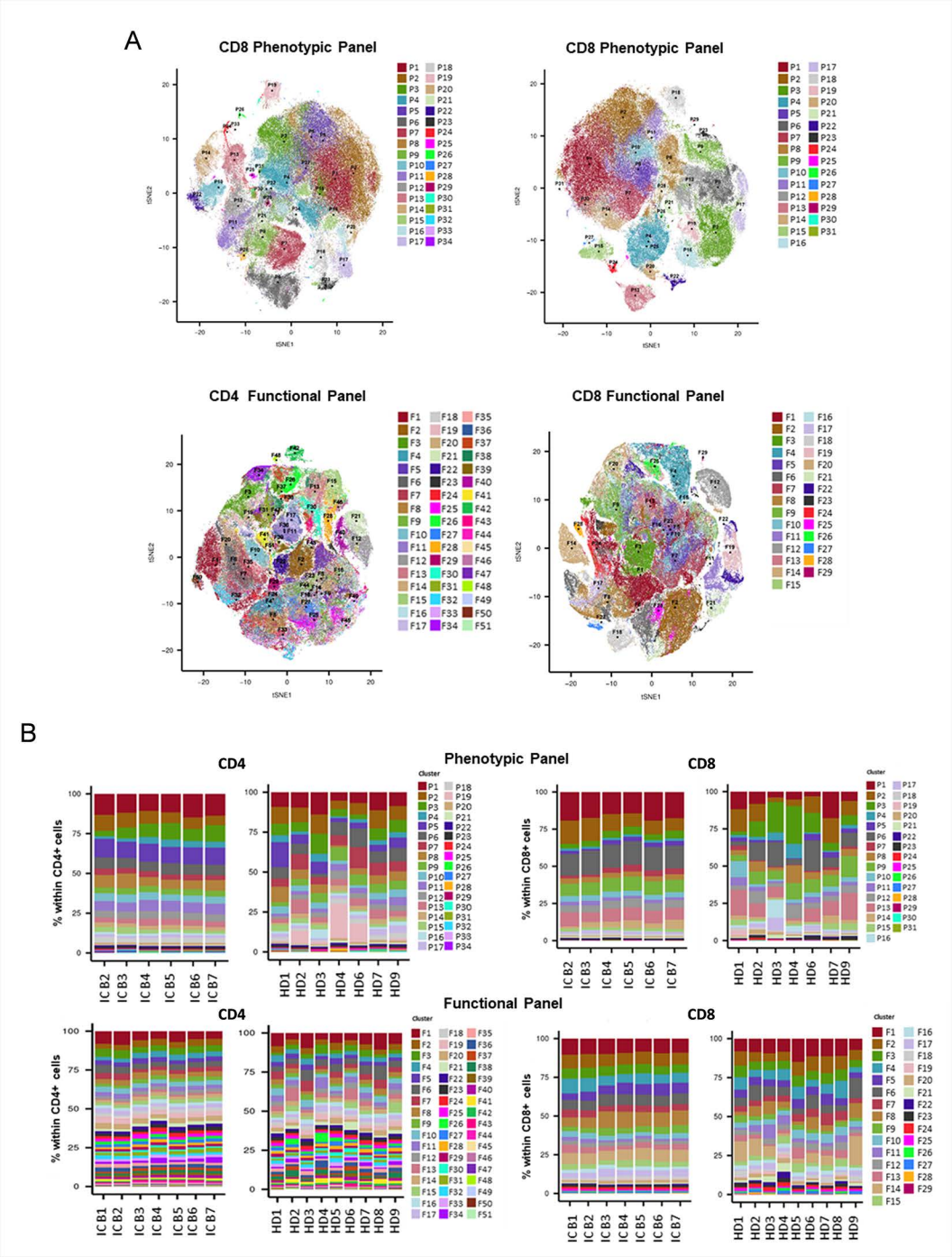
A
CD8 Phenotypic Panel
CD8 Phenotypic Panel
CD4 Functional Panel
CD8 Functional Panel
tSNE1
tSNE2
B
CD4
Phenotypic Panel
CD8
Functional Panel
% within CD4+ cells
% within CD8+ cells
Cluster
IC B2
IC B3
IC B4
IC B5
IC B6
IC B7
IC B1
HD1
HD2
HD3
HD4
HD5
HD6
HD7
HD8
HD9

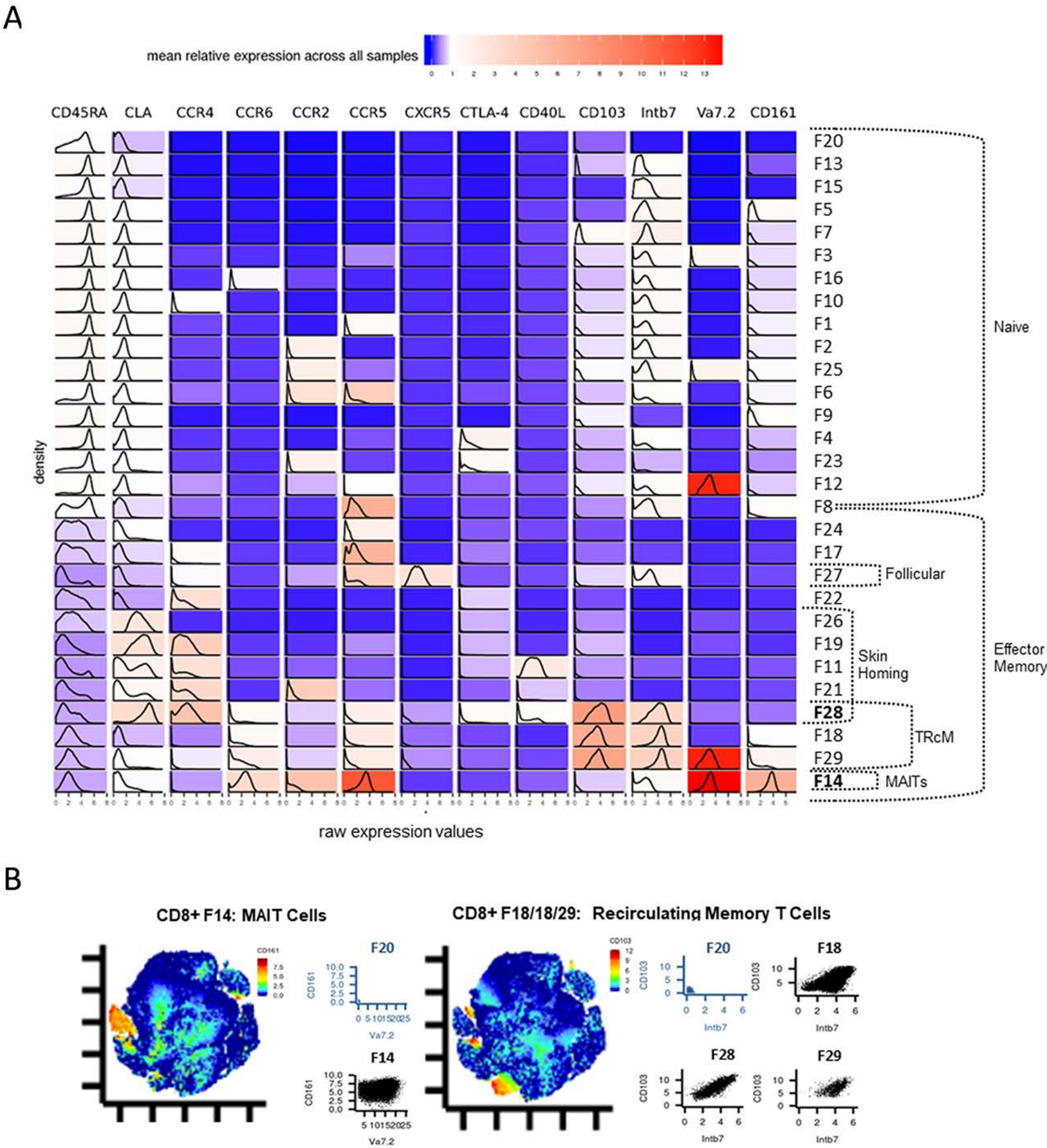
A
mean relative expression across all samples
0 1 2 3 4 5 6 7 8 9 10 11 12 13
CD45RA
CLA
CCR4
CCR6
CCR2
CCR5
CXCR5
CTLA-4
CD40L
CD103
Intb7
Va7.2
CD161
F20
F13
F15
F5
F7
F3
F16
F10
F1
F2
F25
F6
F9
F4
F23
F12
F8
F24
F17
F27
F22
F26
F19
F11
F21
F28
F18
F29
F14
Naive
Follicular
Skin Homing
TRcM
MAITs
Effector Memory
density
0 2 4 6 8
raw expression values
B
CD8+ F14: MAIT Cells
CD161
7.5
5.0
2.5
0.0
F20
CD161
10.0
7.5
5.0
2.5
0.0
0 5 10 15 20 25
Va7.2
F14
CD161
10.0
7.5
5.0
2.5
0.0
5 10 15 20 25
Va7.2
CD8+ F18/18/29: Recirculating Memory T Cells
CD103
12
9
6
3
0
F20
CD103
10
5
0
0 2 4 6
Intb7
F18
CD103
10
5
0 2 4 6
Intb7
F28
CD103
10
5
0
0 2 4 6
Intb7
F29
CD103
10
5
0
0 2 4 6
Intb7

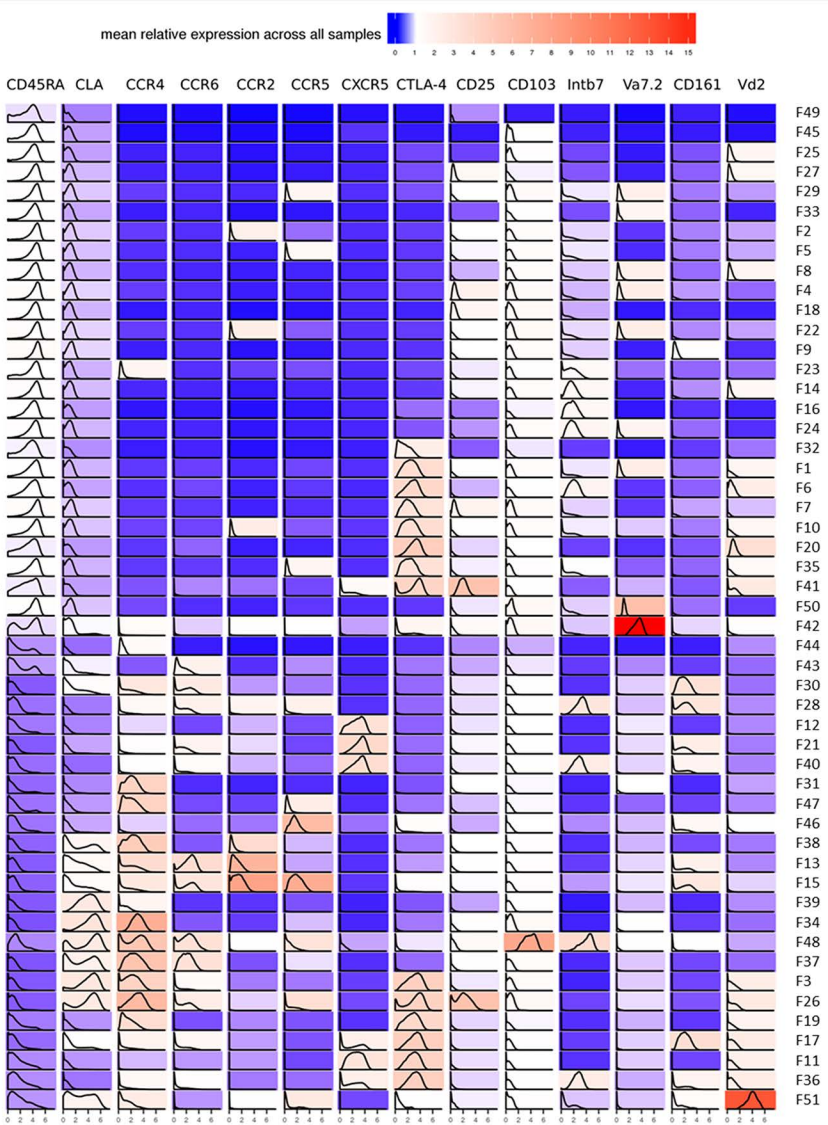
mean relative expression across all samples
0 1 2 3 4 5 6 7 8 9 10 11 12 13 14 15
CD45RA
CLA
CCR4
CCR6
CCR2
CCR5
CXCR5
CTLA-4
CD25
CD103
Intb7
Va7.2
CD161
Vd2
density
F49
F45
F25
F27
F29
F33
F2
F5
F8
F4
F18
F22
F9
F23
F14
F16
F24
F32
F1
F6
F7
F10
F20
F35
F41
F50
F42
F44
F43
F30
F28
F12
F21
F40
F31
F47
F46
F38
F13
F15
F39
F34
F48
F37
F3
F26
F19
F17
F11
F36
F51

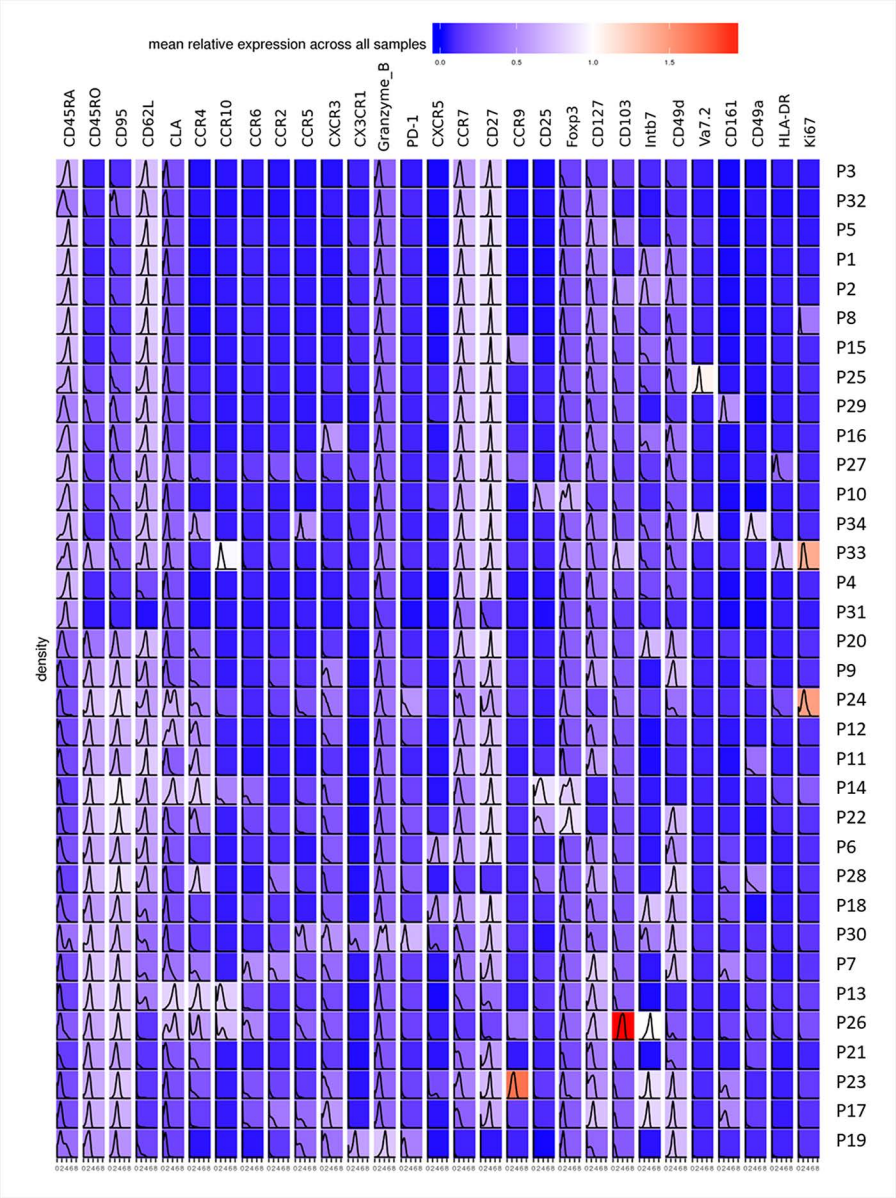
mean relative expression across all samples
0.0
0.5
1.0
1.5
CD45RA
CD45RO
CD95
CD62L
CLA
CCR4
CCR10
CCR6
CCR2
CCR5
CXCR3
CX3CR1
Granzyme_B
PD-1
CXCR5
CCR7
CD27
CCR9
CD25
Foxp3
CD127
CD103
Intb7
CD49d
Va7.2
CD161
CD49a
HLA-DR
Ki67
density
P3
P32
P5
P1
P2
P8
P15
P25
P29
P16
P27
P10
P34
P33
P4
P31
P20
P9
P24
P12
P11
P14
P22
P6
P28
P18
P30
P7
P13
P26
P21
P23
P17
P19
0
2
4
6
8

mean relative expression across all samples
0.0
0.5
1.0
1.5
CD45RA
CD45RO
CD95
CD62L
CLA
CCR4
CCR10
CCR6
CCR2
CCR5
CXCR3
CX3CR1
Granzyme_B
PD-1
CXCR5
CCR7
CD27
CCR9
CD127
CD103
Intb7
CD49d
Va7.2
CD161
CD49a
HLA-DR
Ki67
density
0 2 4 6 8
P14
P1
P7
P8
P2
P10
P5
P30
P11
P18
P31
P29
P28
P6
P3
P19
P17
P23
P9
P21
P22
P12
P13
P4
P25
P26
P20
P24
P27
P15
P16

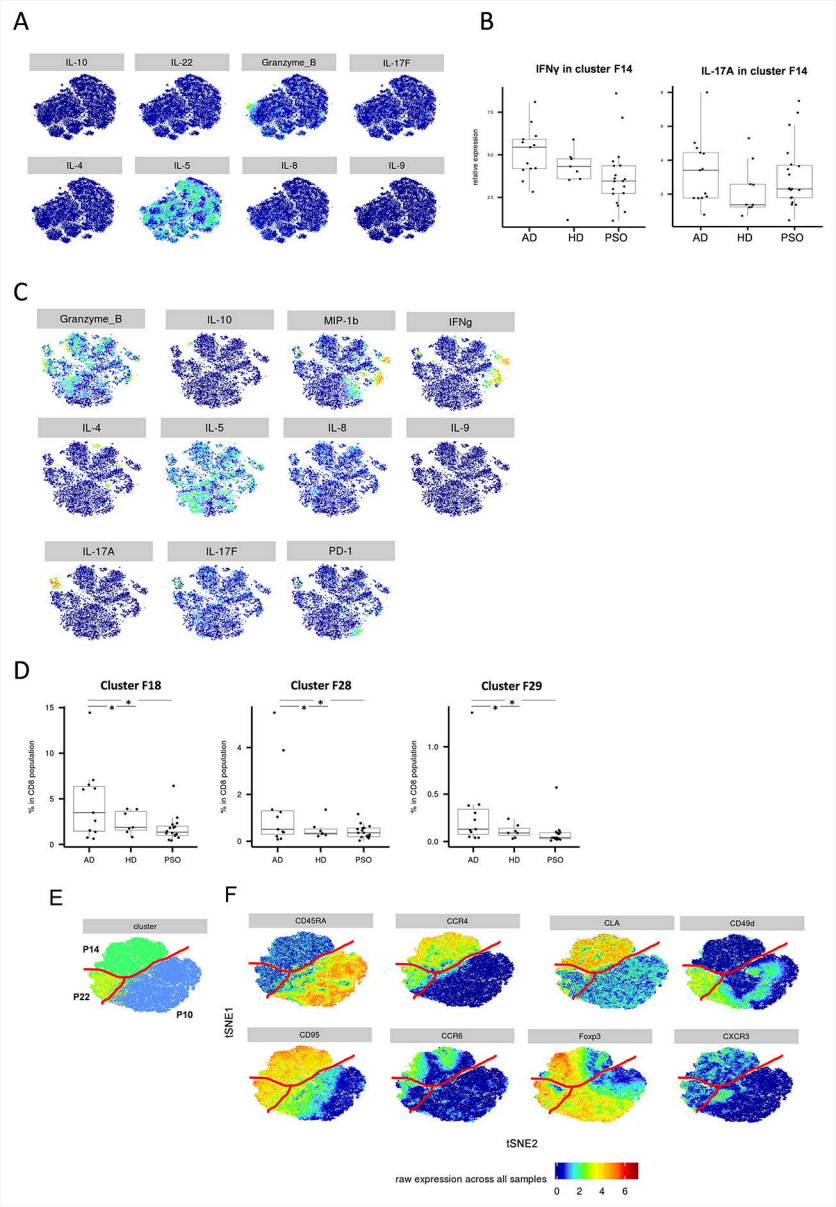
A
IL-10
IL-22
Granzyme_B
IL-17F
IL-4
IL-5
IL-8
IL-9
B
IFNγ in cluster F14
IL-17A in cluster F14
relative expression
AD
HD
PSO
C
Granzyme_B
IL-10
MIP-1b
IFNg
IL-4
IL-5
IL-8
IL-9
IL-17A
IL-17F
PD-1
D
Cluster F18
Cluster F28
Cluster F29
% in CD8 population
E
cluster
P14
P22
P10
F
CD45RA
CCR4
CLA
CD49d
CD95
CCR6
Foxp3
CXCR3
tSNE1
tSNE2
raw expression across all samples
0 2 4 6

Table E1 Demographics and clinical data

Patient	Ethnicity	Age	Sex	Disease onset	Disease phenotype	Disease Severity	Comorbidities	Recurrent Infections	serum IgE (KU/L)	Notes
AD1	Mixed	18	M	not known	Generalised;flexural pattern	SASSAD 30	Asthma, Allergic Rhinocongintivitis	S.aureus; HSV (eczema herpeticum)	23207 ± 2030	Excluded from unsupervised analysis (Phenotypic Panel)
AD2	Black	25	M	Childhood	Follicular/papular phenotype; extensor pattern	not known	Asthma, Allergic Rhinocongintivitis	not known	855 ± 56	Excluded from unsupervised analysis (Phenotypic Panel)
AD3	White	26	M	Childhood	Generalised;flexural pattern	SASSAD 17	Asthma, Allergic Rhinocongintivitis	S.aureus; HSV (eczema herpeticum)	1664 ± 27	Excluded from unsupervised analysis (Phenotypic Panel)
AD4	White	50	M	Childhood	Generalised;flexural pattern	not known	Asthma, Allergic Rhinocongintivitis, Food allergies	not known	83 ± 3	
AD5	White	32	M	Childhood	Generalised;flexural pattern	not known	None	not known	2722 ± 50	
AD6	*White*	*59*	*F*	*Childhood*	*Generalised; flexural prominence*	*SASSAD 31*	*Asthma, Allergic Rhinocongintivitis*	*not known*	*36292 ± 155*	*Excluded from overall analysis for low cell viability*
AD7	Black	57	F	Childhood	Generalised;flexural pattern; hand and foot eczema	SASSAD19	None	S.aureus (abscesses)	1205 ± 15	
AD8	White	47	M	Childhood	Generalised;flexural pattern; hand and foot eczema	SASSAD 24	Asthma, Allergic Rhinocongintivitis	Extensive molluscum contagiosum	5243 ± 175	
AD9	White	49	M	Childhood	Generalised;flexural pattern	SASSAD 27	Asthma, Allergic Rhinocongintivitis	S.aureus; HSV (eczema herpeticum)	1118 ± 58	
AD10	White	35	M	not known	Generalised;flexural pattern	not known	Asthma, food allergies	HSV (eczema herpeticum)	5452 ± 55	
AD11	White	60	M	Adult	Generalised;flexural pattern; hand eczema	SASSAD17	Metals allergy	not known	243 ±4	
AD12	Black	40	M	Childhood	Generalised;flexural pattern	SASSAD 20	Asthma, Allergic Rhinocongintivitis	not known	1318 ± 36	
AD13	Asian	30	M	not known	Generalised;flexural pattern; hand eczema	SASSAD 15	Allergic Rhinocongintivitis	S.aureus	757 ± 5	
AD14	Asian	65	M	not known	Generalised;flexural pattern	SASSAD21	Allergic Rhinocongintivitis	S.aureus; HSV (eczema herpeticum)	6516 ± 172	
AD15	Asian	36	M	not known	Generalised;flexural pattern; hand eczema	SASSAD 15	None	S.aureus	17654 ±724	
PSO1	White	27	M	Teenager	Plaque-psoriasis	PASI 10.5	Psoriatic arthritis	not applicable	not applicable	Excluded from unsupervised analysis (Phenotypic Panel)
PSO2	White	48	M	Adult	Plaque-psoriasis	PASI 21.2	none	not applicable	not applicable	
PSO3	White	40	M	Childhood	Plaque-psoriasis	PASI 10.2	none	not applicable	not applicable	
PSO4	White	37	F	Childhood	Plaque-psoriasis	PASI 23.3	none	not applicable	not applicable	
PSO5	White	37	M	Adult	Plaque-psoriasis	PASI 12.8	none	not applicable	not applicable	
PSO6	White	50	M	Adult	Plaque-psoriasis	PASI 33.4	liver disease	not applicable	not applicable	
PSO7	White	53	F	Teenager	Plaque-psoriasis	PASI 14.1	none	not applicable	not applicable	
PSO8	White	58	F	Childhood	Plaque-psoriasis	PASI 9.9	none	not applicable	not applicable	Excluded from unsupervised analysis (Phenotypic Panel)

PSO9	White	47	M	Teenager	Plaque-psoriasis	PASI 17.3	none	not applicable	not applicable	
PSO10	White	50	M	Adult	Plaque-psoriasis	PASI 15.3	Hyperthension, hypercolerestemia	not applicable	not applicable	
PSO11	Asian	19	M	Childhood	Plaque-psoriasis	PASI 22.7	none	not applicable	not applicable	Excluded from the analysis of Phenotypic markers
PSO12	Asian	37	M	Childhood	Plaque-psoriasis	PASI 17.9	none	not applicable	not applicable	
PSO13	White	48	M	Adult	Plaque-psoriasis	PASI 12.6	none	not applicable	not applicable	
PSO14	White	45	M	Teenager	Plaque-psoriasis	PASI 25	none	not applicable	not applicable	
PSO15	Asian	28	M	Teenager	Plaque-psoriasis	PASI 35.5	none	not applicable	not applicable	
PSO16	White	36	F	Adult	Plaque-psoriasis	PASI 17.6		not applicable	not applicable	
PSO17	White	61	F	Adult	Plaque-psoriasis	PASI 13.5	asthma	not applicable	not applicable	
PSO18	White	33	F	Adult	Plaque-psoriasis	PASI 13.7	asthma	not applicable	not applicable	
PSO19	White	35	F	Adult	Plaque-psoriasis	PASI 26.7	none	not applicable	not applicable	
HD1	White	50	M	not applicable	not applicable	not applicable	not applicable	not applicable	not applicable	Excluded from the unsuprvised analysis of Phenotypic markers
HD2	White	53	M	NA	NA	NA	NA	NA	NA	Excluded from unsupervised analysis (Phenotypic Panel)
HD3	White	32	M	NA	NA	NA	NA	NA	NA	
HD4	White	28	F	NA	NA	NA	NA	NA	NA	
HD5	White	53	F	NA	NA	NA	NA	NA	NA	
HD6	White	48	M	NA	NA	NA	NA	NA	NA	
HD7	White	31	M	NA	NA	NA	NA	NA	NA	
HD8	White	24	M	NA	NA	NA	NA	NA	NA	
HD9	White	32	M	NA	NA	NA	NA	NA	NA	

Table E2 Staining panels

Phenotypic Panel					Functional Panel			
Metal	**Antibody / Target**	**Company (clone)**	**Staining step**		**Metal**	**Antibody / Target**	**Company (clone)**	**Staining step**
103	Cellular Barcode	Synthesized in house	Surface III		103	Cellular Barcode	Synthesized in house	Surface III
104	Cellular Barcode	Synthesized in house	Surface III		104	Cellular Barcode	Synthesized in house	Surface III
105	Cellular Barcode	Synthesized in house	Surface III		105	Cellular Barcode	Synthesized in house	Surface III
106	Cellular Barcode	Synthesized in house	Surface III		106	Cellular Barcode	Synthesized in house	Surface III
108	Cellular Barcode	Synthesized in house	Surface III		108	Cellular Barcode	Synthesized in house	Surface III
110	Cellular Barcode	Synthesized in house	Surface III		110	Cellular Barcode	Synthesized in house	Surface III
113	Cellular Barcode	Synthesized in house	Surface III		113	Cellular Barcode	Synthesized in house	Surface III
89	CD45	Fluidigm (HI30)	Surface II		89	CD45	Fluidigm (HI30)	Surface II
112/114	Qdot800-CD14	Invitrogen (TuK4)	Surface II		112/114	Qdot800-CD14	Invitrogen (TuK4)	Surface II
115	CD57	Biolegend (HCD57)	Surface II		115	CD57	Biolegend (HCD57)	Surface II
139	TCRγδ PE (Primary)	Invitrogen (5A6.E9)	Surface II		139	TCRγδ PE (Primary)	Invitrogen (5A6.E9)	Surface II
	anti-PE (Secondary)	Biolegend (PE001)				anti-PE (Secondary)	Biolegend (PE001)	
140	CD3	Biolegend (UCHT1)	Surface II		140	CD3	Biolegend (UCHT1)	Surface II
141	HLA-DR	Biolegend (L243)	Surface II		146	CD8α	Biolegend (SK1)	Surface II
142	CLA	Biolegend (HECA-452)	Surface II		147	CD45RA	Biolegend (HI100)	Surface I
143	CD38	Biolegend (HIT2)	Surface II		148	CLA	Biolegend (HECA-452)	Surface II
144	Granzyme B	Abcam (CLB-GB11)	Surface II		149	CD4	Biolegend (SK3)	Surface I
145	CD62L	BD Biosciences (DREG-56)	Surface II		150	CD103	eBioscience (B-Ly7)	Surface I
146	CD8α	Biolegend (SK1)	Surface II		152	CD25	Biolegend (M-A251)	Surface I
147	CD45RO	Biolegend (UCHL1)	Surface II		153	CD107a	BD Biosciences (H4A3)	Surface II
148	Vδ2	Biolegend (B6)	Surface II		154	CD40L	eBioscience (24-31)	Surface II
149	CD4	Biolegend (SK3)	Surface II		155	CTLA-4	BD Biosciences (BNI3)	Surface II
150	CD103	eBioscience (B-Ly7)	Surface II		156	Vδ2	Biolegend (B6)	Surface II
151	CCR4	R&D Systems (205410)	Surface II		158	CD56	BD Biosciences (NCAM16.2)	Surface II
152	Ki-67	BD Biosciences (B56)	Intra		159	Integrin β7	Biolegend (FIB504)	Surface I
153	CD49a	Biolegend (TS2/7)	Surface II		161	CCR9	Biolegend (L053E8)	Surface I

154	CCR10	R&D Systems (314305)	Surface II		163	CD161	Biolegend (HP-3G10)	Surface I
155	Foxp3 Biotin (Primary)	eBioscience (PCH101)	Intra		164	CD19	Biolegend (HIB19)	Surface II
	Streptavidin (Secondary)	Synthesized in house			165	Vα7.2	Biolegend (3C10)	Surface I
156	CCR7	R&D Systems (150503)	Surface I		166	CXCR5	BD Biosciences (RF8B2)	Surface I
157	CD27	eBioscience (LG.7F9)	Surface I		168	CCR2	Biolegend (K036C2)	Surface I
158	CD56	BD Biosciences (NCAM16.2)	Surface II		171	CCR6	Biolegend (G034E3)	Surface I
159	Integrin β7	Biolegend (FIB504)	Surface I		173	CCR4	R&D Systems (205410)	Surface I
160	PD-1	eBioscience (eBioJ105)	Intra		175	CCR5	Abcam (HEK/1/85a)	Surface I
161	Vδ1 FITC (Primary)	Miltenyi Biotec (REA173)	Surface II		209	CD16	Fluidigm (3G8)	Surface II
	anti-FITC (Secondary)	Biolegend (FIT-22)			141	IFN-γ	eBioscience (4S.B3)	Intra
162	CD95	Biolegend (DX2)	Surface II		142	TNF-α	eBioscience (MAb11)	Intra
163	CXCR3	R&D Systems (49801)	Surface II		143	IL-8	Biolegend (E8N1)	Intra
164	CCR9	Biolegend (L053E8)	Surface I		144	Granzyme B	Abcam (CLB-GB11)	Intra
165	Vα7.2	Biolegend (3C10)	Surface I		145	IL-17F	eBioscience (SHLR17)	Intra
166	CXCR5	BD Biosciences (RF8B2)	Surface II		151	IL-2	eBioscience (MQ1-17H12)	Intra
167	CD49d	Biolegend (9F10)	Surface II		157	MIP-1β	BD Biosciences (D21-1351)	Intra
168	CCR2	Biolegend (K036C2)	Surface I		160	PD-1	eBioscience (eBioJ105)	Intra
169	CD25	Biolegend (M-A251)	Surface II		162	IL-5	Biolegend (JES1-39D10)	Intra
170	CD161	Biolegend (HP-3G10)	Surface I		167	IL-9	BD Biosciences (MH9A4)	Intra
171	CCR6	Biolegend (G034E3)	Surface II		169	IL-4	Biolegend (MP4-25D2)	Intra
172	CD45RA	Biolegend (HI100)	Surface II		170	IL-10	eBioscience (JES3-9D7)	Intra
173	CD19	Biolegend (HIB19)	Surface II		172	GM-CSF	Biolegend (BVD2-21C11)	Intra
174	CX3CR1	Biolegend (K0124E1)	Surface II		174	IL-22	Biolegend (Poly5161)	Intra
175	CCR5	Abcam (HEK/1/85a)	Surface I		176	IL-17A	Biolegend (BL168)	Intra
176	CD127	Biolegend (A019D5)	Surface II		191/193	DNA	Fluidigm	DNA
209	CD16	Fluidigm (3G8)	Surface II		195	CisPlatin	Sigma-Aldrich	Live/dead
191/193	DNA	Fluidigm	DNA					
195	CisPlatin	Sigma-Aldrich	Live/dead					

Table E3 Class Comparisons

Variable	Two-way comparisons	Dataset	Cluster (-Cytokine)	adj p value	Estimate	Interpretation
Cell Frequency	AD vs HD	CD8+ Phenotypic	P15	0.01918	5.4545	TRcM ↑ in AD
			P27	0.04711	0.3009	TRcM ↑ in AD
			P24	0.04711	1.2636	TRcM ↑ in AD
		CD8+ Functional	F18	0.03012	3.7208	TRcM ↑ in AD
			F28	0.04756	1.3014	TRcM ↑ in AD
			F29	0.04756	0.2971	TRcM ↑ in AD
	Pso vs AD	CD4+ Phenotypic	P22	0.02238	0.597	CD49d+ Tregs ↓ in AD
		CD8+ Phenotypic	P15	0.00688	-4.8345	TRcM ↑ in AD
			P27	0.00688	-0.2957	TRcM ↑ in AD
			P13	0.00688	-5.3525	MAITs ↓ in Pso
			P24	0.00688	-1.2771	TRcM ↑ in AD
			P8	0.03115	3.2531	
		CD8+ Functional	F18	0.02473	-3.4072	TRcM ↑ in AD
			F28	0.02473	-1.3535	TRcM ↑ in AD
			F29	0.04425	-0.2861	TRcM ↑ in AD
	Pso vs HD	CD8+ Phenotypic	P13	0.02057	-5.159	MAITs ↓ in Pso
			P18	0.01999	1.3257	
			P3	0.02057	-11.2144	
		CD8+ Functional	F6	0.01198	-2.6657	
			F1	0.01198	-3.0584	
Cytokine expression	AD vs HD	CD8+ Functional	F28-IL-22	0.0346	4.6189	↑ IL-22 Skin homing TRcM in AD
	Pso vs AD	CD4+ Functional	F36-IL-2	8.96E-07	-1.6209	
			F17-IL-2	0.00076	-1.4239	
			F15-IL-5	0.00076	-0.1376	
			F20-IL-2	0.0016	-0.9294	
			F6-IL-2	0.00189	-0.8553	
			F1-IL-2	0.00189	-0.7572	
			F17-IL-4	0.00331	-1.0255	
			F10-IL-2	0.00413	-0.7834	
			F15-GM-CSF	0.00413	-2.87	
			F35-IL-2	0.00413	-0.8284	
			F28-IL-2	0.00413	-2.1091	
			F15-IL-2	0.00446	-1.5149	
			F3-Granzyme_B	0.00489	-0.274	
			F7-IL-2	0.00526	-0.7901	

			F34-Granzyme_B	0.00551	-0.4253	
			F26-TNFα	0.00555	-0.4811	
			F17-IL-10	0.00583	-1.0828	
			F3-IL-17F	0.00634	-0.3753	
			F26-IL-2	0.00847	-0.9284	CD4+ T cells more activated in AD
			F26-GM-CSF	0.00859	-2.1144	
			F15-IL-4	0.00905	-1.4349	
			F26-Granzyme_B	0.00958	-0.2734	
			F3-TNF	0.01183	-0.5216	
			F48-GM-CSF	0.01221	-5.5909	
			F11-IL-2	0.01292	-1.1134	
			F19-IL-2	0.01292	-1.5154	
			F34-IL-22	0.01356	-1.2253	
			F40-IL-2	0.01523	-1.4544	
			F28-GM-CSF	0.01745	-3.1101	
			F32-IL-2	0.01745	-0.7572	
			F17-TNF	0.02153	-0.4009	
			F3-IL-2	0.02316	-1.4063	
			F1-IL-17F	0.02316	-0.0657	
			F17-GM-CSF	0.02341	-0.6456	
			F26-IL-22	0.03003	-0.9507	
			F21-IL-2	0.03239	-1.3264	
			F36-IL-5	0.04464	-0.0782	
		CD8+ Functional	F14-TNFα	0.01791	-0.8907	MAITs more activated in AD
			F14-MIP1β	0.03995	-1.1912	
	Pso vs HD	CD4+ Functional	F15-IL-4	0.01818	-1.6613	CD4+ T cells not over-activated in PSO
			F47-IFNγ	0.0293	-2.218	
			F47-MIP-1β	0.0293	-0.7495	
			F40-IFNγ	0.0293	-0.4006	
			F28-IL-4	0.0293	-1.849	
			F31-IFNγ	0.0293	-0.6983	
			F44-MIP-1β	0.04397	-0.6579	
			F44-GM-CSF	0.04397	-1.113	

Table E4 Markers used for clustering

Clustering markers							
Functional CD4 dataset		Functional CD8 dataset		Phenotypic CD4 dataset		Phenotypic CD8 dataset	
147	CD45RA	147	CD45RA	172	CD45RA	172	CD45RA
148	CLA	148	CLA	142	CLA	142	CLA
150	CD103	150	CD103	150	CD103 (αε Integrin)	150	CD103 (αε Integrin)
152	CD25	155	CTLA-4	169	CD25	159	Integrinβ7
155	CTLA-4	159	Integrinβ7	159	Integrinβ7	170	CD161
156	Vd2	163	CD161	170	CD161	165	Va7.2
159	Integrinβ7	165	Va7.2	165	Va7.2	166	CXCR5
163	CD161	166	CXCR5	166	CXCR5	168	CCR2
165	Va7.2	168	CCR2	168	CCR2	171	CCR6
166	CXCR5	171	CCR6	171	CCR6	151	CCR4
168	CCR2	173	CCR4	151	CCR4	175	CCR5
171	CCR6	175	CCR5	175	CCR5	145	CD62L
173	CCR4	154	CD40L	145	CD62L	141	HLA-DR
175	CCR5			141	HLA-DR	147	CD45RO
				147	CD45RO	144	Granzyme B
K value				144	Granzyme B	152	Ki67
K=10		*K=100*		152	Ki67	153	CD49a (α1 Integrin)
				153	CD49a (α1 Integrin)	154	CCR10
				154	CCR10	156	CCR7
				155	Foxp3	157	CD27
				156	CCR7	160	PD-1
				157	CD27	162	CD95
				160	PD-1	163	CXCR3
				162	CD95	164	CCR9
				163	CXCR3	167	CD49d (α4 Integrin)
				164	CCR9	174	CX3CR1
				167	CD49d (α4 Integrin)	176	CD127
				174	CX3CR1		
				176	CD127		
				K value			
				K=10		*K=25*	